Resveratrol Attenuates Intermittent Hypoxia-Induced Macrophage Migration to Visceral White Adipose Tissue and Insulin Resistance in Male Mice

Alba Carreras, Shelley X. L. Zhang, Isaac Almendros, Yang Wang, Eduard Peris, Zhuanhong Qiao, and David Gozal

Section of Pediatric Sleep Medicine, Department of Pediatrics, Comer Children's Hospital, Pritzker School of Medicine, The University of Chicago, Chicago, Illinois 60637

Chronic intermittent hypoxia during sleep (IH), as occurs in sleep apnea, promotes systemic insulin resistance. Resveratrol (Resv) has been reported to ameliorate high-fat diet-induced obesity, inflammation, and insulin resistance. To examine the effect of Resv on IH-induced metabolic dysfunction, male mice were subjected to IH or room air conditions for 8 weeks and treated with either Resv or vehicle (Veh). Fasting plasma levels of glucose, insulin, and leptin were obtained, homeostatic model assessment of insulin resistance index levels were calculated, and insulin sensitivity tests (phosphorylated AKT [also known as protein kinase B]/total AKT) were performed in 2 visceral white adipose tissue (VWAT) depots (epididymal [Epi] and mesenteric [Mes]) along with flow cytometry assessments for VWAT macrophages and phenotypes (M1 and M2). IH-Veh and IH-Resv mice showed initial reductions in food intake with later recovery, with resultant lower body weights after 8 weeks but with IH-Resv showing better increases in body weight vs IH-Veh. IH-Veh and IH-Resv mice exhibited lower fasting glucose levels, but only IH-Veh had increased homeostatic model assessment of insulin resistance index vs all 3 other groups. Leptin levels were preserved in IH-Veh but were significantly lower in IH-Resv. Reduced VWAT phosphorylated-AKT/AKT responses to insulin emerged in both Mes and Epi in IH-Veh but normalized in IH-Resv. Increases total macrophage counts and in M1 to M2 ratios occurred in IH-Veh Mes and Epi compared all other 3 groups. Thus, Resv ameliorates food intake and weight gain during IH exposures and markedly attenuates VWAT inflammation and insulin resistance, thereby providing a potentially useful adjunctive therapy for metabolic morbidity in the context of sleep apnea. **(*Endocrinology* 156: 437–443, 2015)**

Intermittent hypoxia during sleep (IH) is one of the hallmarks of obstructive sleep apnea (OSA) and induces a wide range of morbid consequences, including excessive daytime sleepiness and cognitive, mood, and neurobehavioral deficits (1–6), as well as cardiovascular dysfunction (7–10). IH also imposes adverse metabolic consequences, such as hyperlipidemia and insulin resistance, even in lean mice, along with structural and cellular remodeling of adipose tissue (11–18). The metabolic consequences of sleep apnea have been causally linked to increased prevalence and clinical deterioration of type 2 diabetes as well as with increased homeostatic model assessment of insulin resistance index (HOMA) in both children and adults (19–24). Furthermore, acute exposures to IH in healthy human subjects elicited alterations in insulin sensitivity (24). However, the mechanisms underlying these alterations remain incompletely elucidated. Evidence indicates that disruption of pancreatic β-cell function and integrity may be operational in IH-induced alterations in glucose homeostasis (25–27) but is insufficient to account for the systemic and tissue-specific insulin resistance, such as seen in adipose tissue (28). Globally, it is currently assumed that the altered insulin sensitivity can be ascribed to IH-induced increases in oxidative stress and activation of inflamma-

ISSN Print 0013-7227 ISSN Online 1945-7170
Printed in U.S.A.

Received August 21, 2014. Accepted November 12, 2014.
First Published Online November 18, 2014

Abbreviations: Akt, protein kinase B; Epi, epididymal; FiO_2, fractional inspired oxygen concentration; HOMA, homeostatic model assessment of insulin resistance index; IH, intermittent hypoxia during sleep; Mes, mesenteric; OSA, obstructive sleep apnea; RA, room air; Resv, resveratrol; SVF, stromal-vascular fraction; Veh, vehicle; VWAT, visceral white adipose tissue.

tory pathways that lead to heightened sympathetic tone, and altered cardiovascular and metabolic parameters, as well as manifesting as a prooxidative status (eg, increased lipid peroxides, enhanced nicotinamide adenine dinucleotide phosphate oxidase, mitochondrial dysfunction, and diminished activities of superoxide dismutases), and augmented inflammatory status (11, 30–32).

In the last decade, resveratrol (Resv) has emerged as potent antiobesogenic compound that affords protection against high-fat-diet-induced obesity and insulin resistance (33–35). Although the mechanisms underlying Resv-induced beneficial effects on systemic and tissue-specific insulin sensitivity remain to be fully delineated, beneficial effects of Resv have emerged on aging, inflammation, and metabolism and are putatively ascribed to activation of the lysine deacetylase, sirtuin 1, cAMP, or AMP-activated protein kinase pathways (36–38). We hypothesized that administration of this compound would dampen IH-induced systemic insulin resistance and potentially reduce visceral white adipose tissue (VWAT) macrophage infiltration and, thus, attenuate insulin resistance in adipocytes.

Materials and Methods

Animals

Adult male C57BL/6J mice from Jackson Laboratories (8 wk old, ~22 g), were housed in groups of 5 (to prevent isolation stress) in standard clear polycarbonate cages and allowed to acclimatize to their surroundings. Mice were fed normal chow diet and water ad libitum and maintained in a 12-hour light, 12-hour dark cycle (light on 7 AM to 7 PM) at a constant temperature (26 ± 1°C). Mice were randomly assigned to IH exposures or room air (RA) conditions and to treatment with Resv or vehicle (Veh) (control) for 8 weeks.

Mice received drinking water containing 0.01% Resv (Sigma-Aldrich). This amount of Resv is approximately 10 times the amount found in 1 L of red wine and was initially dissolved in 0.4 mL of absolute ethanol and then added to 100 mL of drinking water. The Veh group received the same volume of drinking water containing an identical concentration of ethanol. All mice had free access to the drinking solution, and mice consumed 3–4 mL of the drinking fluid daily, with the daily consumption of Resv being 0.3–0.4 mg/mouse (ie, a relatively high dose of the compound with demonstrated efficacy) (39).

Animal experiments were performed according to protocols approved by the Institutional Animal Committee University of Chicago of the University of Chicago and are in close agreement with the National Institutes of Health Guide in the Care and Use of Animals. All efforts were made to minimize animal suffering and to reduce the number of animals used.

Intermittent hypoxia exposures

Mice were placed in identical commercially designed chambers (30 × 20 × 20 inches; Oxycycler A44XO; BioSpherix) operated under a 12-hour light, 12-hour dark cycle (7 AM to 7 PM) for a period of 8 weeks. Programmed gas concentrations were circulated into each chamber, and an internal O_2 analyzer measured the O_2 concentration continuously. Deviations from the fixed concentrations were automatically corrected by a computerized system of solenoid valves controlling gas outlets adding either N_2 or O_2. Ambient CO_2 in the chamber was maintained at less than 0.01%, and humidity was also maintained at 40%–50% by circulating the gas through a freezer and silica gel. Ambient temperature was kept at 26°C as described previously by Gozal and coworkers (1, 15) and Gozal et al (40). Mice were subjected for 12 hours during daylight to intermittent hypoxia/normoxia cycles of 3-minute duration (hypoxia, nadir of FiO_2: 6.4% for 90 s alternating with normoxia [fractional inspired oxygen concentration, FiO_2, 21%] for 90 s). This IH profile is associated with reproducible nadir of oxyhemoglobin saturations in the 65%–72% range. Normoxic (FiO_2, 21%) conditions were used during the 12-hour lights-off period. Control animals were exposed to circulating RA (FiO_2, 21%) during daylight and lights-off period.

Food consumption and body weight

Food consumption per cage was registered daily, always at the same time of the day (middle of the light period). Animal food consumption was then calculated by dividing the daily cage chow use by the number of mice in the cage. Body weight was measured every other day always at the same time of the day (middle of the light cycle period). Body weight gain was determined by subtracting the body weight on first day of IH exposure from the body weight on subsequent days.

ELISA and insulin sensitivity assays

Mice were fasted for 3 hours (4–7 AM) with water available ad libitum and were then euthanized. Venous blood was collected into EDTA-containing tubes, immediately centrifuged in at 4°C, and frozen at −80°C until further analyses. Blood glucose was immediately assessed using an OneTouch Ultra2 glucometer (Life Scan, Inc). Insulin and leptin assays were carried out using ELISA kits (Millipore) according to the manufacturer's protocol. The linear range of the insulin assay was 0.2–10 ng/mL, with the limit of sensitivity at 0.2 ng/mL (35pM) and intra- and interindividual coefficients of variation up to 8.8% and 17.6%, respectively, at lower concentrations (ie, 0.32 ng/mL). Similarly for the leptin assay, the linear range was 0.2 up to 30 ng/mL with the sensitivity threshold at 0.05 ng/mL (~3.13pM). The intraassay variation coefficient was up to 1.7% at high concentrations of leptin (17.60 ng/mL) and 6.8% of interindividual coefficient of variation at low concentrations (ie, 1.66 ng/mL). The homeostatic model (HOMA) was then calculated as the product of glucose and insulin levels divided by 405.

Adipocyte insulin sensitivity was assessed in adipocytes derived from epididymal (Epi) and mesenteric (Mes) fat tissue depots as described previously (41). Briefly, primary adipocytes were isolated by collagenase digestion and flotation centrifugation. They were then incubated with insulin at various concentrations at 37°C for 10 minutes with gentle vortexing every 2 minutes. After 2 washes with cold Krebs-Ringer buffer, cells were lysed in Laemmli buffer and assessed using Western blot analysis for phosphorylated and total Akt (protein kinase B)

Table 1. Information on All Antibodies and Reagents Used in Current Study

Treg			
CD3-FITC	Clone 145-2C11	100306	Biolegend
CD4-PE	Clone RM4-4	116006	Biolegend
CD8-APC/Cy7	Clone 53-6.7	100714	Biolegend
CD25-PerCP/Cy5.5	Clone PC61	102030	Biolegend
FoxP3-APC	Clone FJK-16s	17-5773	eBioscience
Macrophages			
CD11b-PB	Clone M1/70	101224	Biolegend
F4/80-PE/Cy7	Clone BM8	123113	Biolegend
CD11c-APC/Cy7	Clone N418	117324	Biolegend
CD206-PE	Clone C068C2	141705	Biolegend
Gr1-PerCP	Clone RB6-8C5	108428	Biolegend
WBC			
CD3-FITC	Clone 145-2C11	100306	Biolegend
CD4-PE	Clone RM4-4	116006	Biolegend
CD8-APC/Cy7	Clone 53-6.7	100714	Biolegend
Gr1-PerCP	Clone RB6-8C5	108428	Biolegend
CD115-APC	Clone AFS98	135509	Biolegend
CD11b-PB	Clone M1/70	101224	Biolegend
CD4-PE	Clone RM4-4	116006	Biolegend
CD8-APC/Cy7	Clone 53-6.7	100714	Biolegend
CD25-PerCP/Cy5.5	Clone PC61	102030	Biolegend
FoxP3-APC	Clone FJK-16s	17-5773	eBioscience

(antiphospho-Akt [Ser473] and anti-Akt; Cell Signaling Technology).

Isolation of stromal-vascular fraction (SVF) and flow cytometry analysis

Epi fat pads and Mes adipose tissues were dissected, isolated, and then minced in Krebs-Ringer buffer supplemented with 1% BSA followed by incubation with collagenase (1 mg/mL; Worthington Biochemical Corp) at 37°C for 45 minutes with shaking. Cell suspensions were filtered through a 100-μm mesh and centrifuged at 500*g* for 5 minutes to separate floating adipocytes from the SVF pellet. SVF pellets were then resuspended in flow cytometry buffer (PBS plus 2% fetal bovine serum), and 10^6 cells were used for staining with fluorescence-conjugate primary antibodies or control IgGs at 4°C for 30 minutes. Cells were then washed twice and analyzed with a flow cytometer (Canto II; BD Biosciences). Data analysis was performed using the FlowJo software (Tree Star). Adipose tissue macrophages were defined as F4/80+ and CD11b+ cells, from which M1 and M2 macrophages were identified as CD11c+ or CD206+ cells, respectively. Please see Table 1 for list of antibody reagents.

Statistical analysis

All values are expressed as mean ± SD. ANOVA procedures followed by post hoc tests and Student's *t* tests were used to compare the results between 4 treatment groups as appropriate, using SPSS statistical software (version 21.0; SPPS, Inc). In all cases, 2-tailed $P < .05$ was considered to achieve statistical significance.

Results

Food intake and weight gain

Mice exposed to IH exhibited initial decreases in food intake that began within the first 24 hours after the initiation of IH and were followed by progressive recovery to control levels within the first week (n = 12/condition;

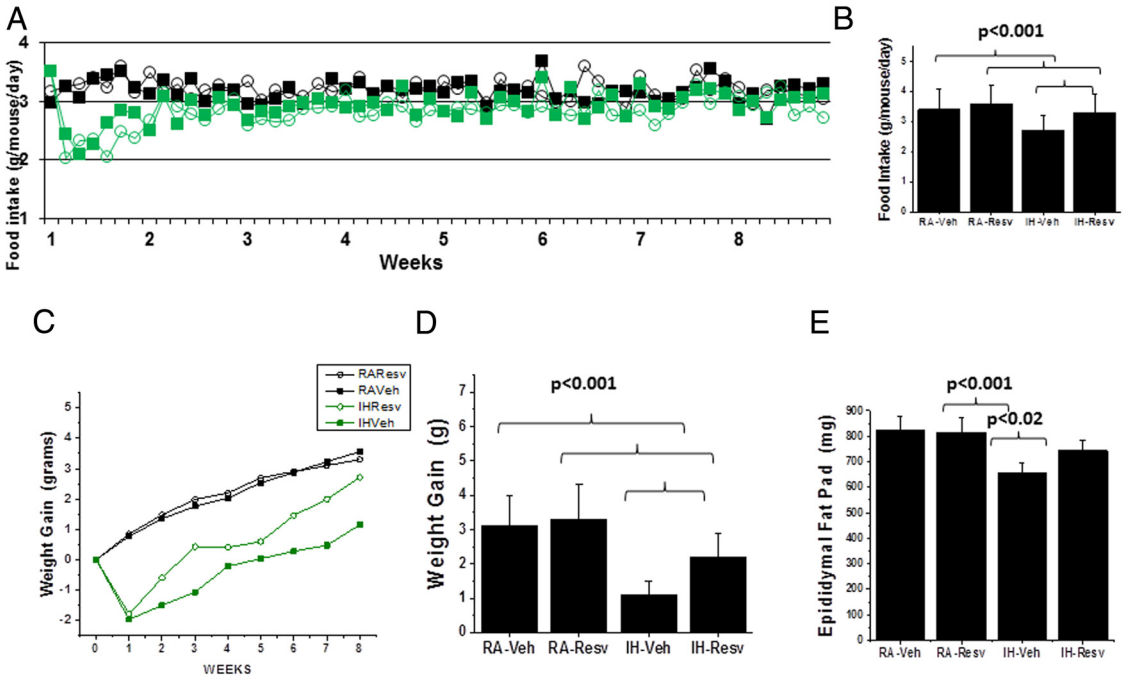

Figure 1. Food intake and weight gain in IH and RA-exposed mice treated with either Resv or Veh for 8 weeks. A, Mean food intake per mouse/d over 8 weeks; green color indicates IH and open circles indicate Resv treatment. Two-way ANOVA (treatment × condition) *F* statistic = 8.18; $P < .001$. B, Mean overall daily food intake for the 8-week period per mouse; $P < .001$. C, Mean weekly changes in body weight over the 8-week period; two-way ANOVA (treatment × condition) *F* statistic = 12.74; $P < .001$. D, Overall changes in body weight; $P < .001$. E, Mean weights of Epi fat pads; $P < .001$, n = 12–24/treatment group.

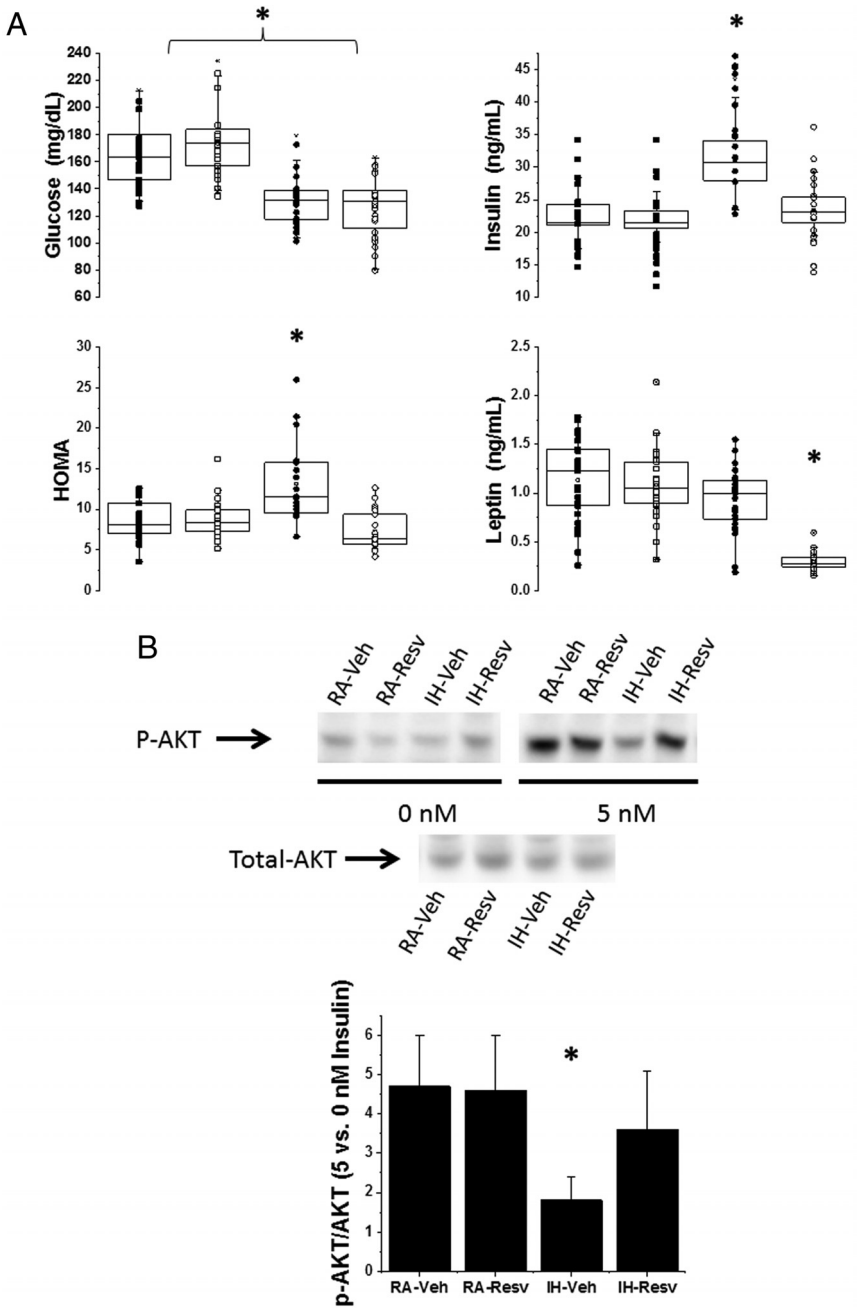

Figure 2. Metabolic effects of Resv in mice. A, Plasma levels of glucose, insulin, and leptin in IH and RA-exposed mice after fasting for 3 hours and treated with either Resv or Veh for 8 weeks. B, Example of Epi adipose tissue insulin sensitivity assay as demonstrated by changes in phosphorylated Akt (p-AKT) and total Akt (total-AKT) after adding 0nM or 5nM insulin to the medium (upper panel). The lower panel illustrates the summary of 6 separate experiments for p-AKT to total-AKT ratios between 0nM and 5nM insulin. Two-way ANOVA: *, $P < .01$ IH-Veh vs 3 other treatment groups. Please note that the findings for Mes adipose tissue were nearly identical (data not shown).

$P < .001$) (Figure 1A). However, IH-Veh-exposed mice showed overall reduced food intake compared with all 3 other groups (Figure 1B). IH-Veh mice displayed poorest weight at the end of the 8-week period, with IH-Resv-exposed mice showing improved weight gain, albeit still lower than RA-treated mice (n = 24 mice/treatment group; $P < .001$) (Figure 1, C and D). Notably, IH-Veh-exposed mice showed most significant reductions in epididymis fat pad weights with some recovery occurring in IH-Resv (n = 12/group) (Figure 1E).

Effect of Resv on systemic insulin and leptin levels and on visceral adipose tissue insulin resistance

Overall fasting glycemic levels were similar across the 4 treatment groups. However, in IH-Veh mice, higher fasting HOMA levels due to higher insulin levels emerged after 8 weeks of IH, with such changes being abrogated in IH-Resv-treated mice (Figure 2). Similarly, plasma leptin levels were unaltered in IH-Veh mice compared with RA-exposed groups, but IH-Rev mice showed markedly reduced plasma leptin levels (Figure 2).

Insulin sensitivity in VWAT, as assessed by Akt phosphorylation in response to insulin in both Mes and Epi adipose tissue depots, indicated the presence of insulin resistance after 8 weeks of IH but only in IH-Veh-treated mice. Overall, the findings were very similar for either Mes or Epi. In contrast, there were significant improvements in adipose tissue insulin sensitivity in IH-exposed mice treated with Resv (n = 8/treatment group) (Figure 2).

Resv protects from IH-induced increases in macrophages and polarization in VWAT

IH for a period of 8 weeks induced marked increases in the global number of macrophages present in the SVF of both Mes and Epi (Figure 3). Such increases consisted primarily of increases in the proportion of macrophages exhibiting the proinflammatory M1 phenotype (CD11c+; n = 8/group, $P < .01$) (Figure 3) and reciprocal reductions in macrophages with M2 polarity (CD206+; n = 8/group, $P < .01$) (Figure 3), such that the M1 to M2 ratio was markedly increased after IH (n = 8/group; $P < .01$) (Figure 3). IH-induced changes

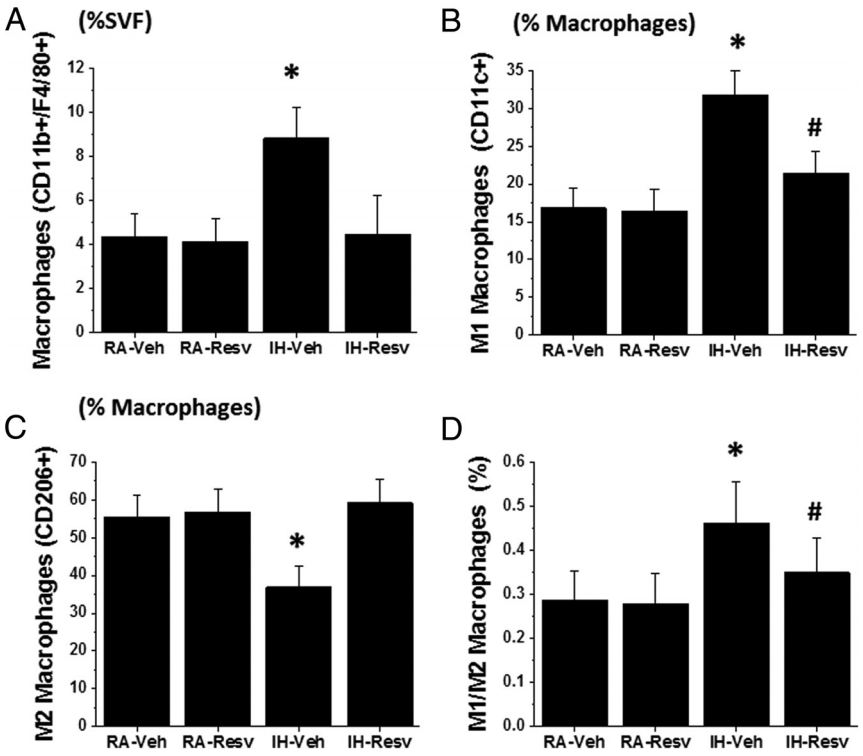

Figure 3. Macrophage cell recruitment in SVF of VWAT in IH and RA-exposed mice treated with either Resv or Veh for 8 weeks. A, Total macrophage count expressed as percentage of cells isolated from SVF. B, M1 macrophage count expressed as percentage of total macrophage count. C, M2 macrophage count expressed as percentage of total macrophage count. D, M1 to M2 ratio. n = 8/experimental group; two-way ANOVA: *, $P < .01$ IH-Veh vs 3 other treatment groups; #, IH-Resv vs RA groups.

in Mes and Epi VWAT depot macrophages were markedly attenuated in Resv-treated mice exposed to IH.

Discussion

This study confirms previous findings that chronic IH exposures imposed during the predominant sleep period in mice lead to the emergence of systemic insulin resistance and increased VWAT inflammation (11–18). Furthermore, we now show that treatment with Resv improved the reduced food intake patterns and weight gain associated with IH-exposures and restored insulin responsiveness while normalizing the inflammatory processes within VWAT depots. Furthermore, Resv administration was associated with marked reductions in circulating leptin levels, suggesting increased leptin receptor sensitivity.

Before we discuss some of the major implications of our findings, some methodological issues deserve specific mention. First, we have implemented an IH experimental paradigm that provides highly reproducible findings and, most importantly, mimics frequently encountered patterns of episodic hypoxia occurring in diseases such as OSA (15). In this context, the initial prominent reductions in food consumption and overall diminished nutrient intake exhibited by IH-exposed mice is similar to that previously reported by us (15) as well as by others (42) and may reflect relative leptin receptor resistance induced by IH in the context of an overall catabolic state (43). Notably, Resv treatment improved IH-mediated deceleration in weight gain during the duration of the experiments, suggesting that the both central and peripheral metabolic and orexigenic pathways modulated by IH are affected by this compound, an effect that is not apparent during normoxic conditions. Secondly, as in previous studies (15), we opted not to expose mice to a high-fat diet regimen or to use transgenic mouse models of obesity or insulin resistance, because we aimed to examine the isolated effects of Resv on IH-induced metabolic dysfunction. Thirdly, we exposed our mice to a realistic and implementable yet relatively higher dose of Resv that has already exhibited favorable outcomes in either metabolic or low-grade chronic inflammatory processes (44–47). There is no doubt that future studies, possibly in patients with sleep apnea, can investigate whether Rev supplements at lower doses effectively translate into similar results as those described here. Finally, we should point out that this study was observational in nature and therefore does not provide insights into which of the multiple mechanisms that have been attributed to Resv effects (33–39) was predominantly involved in current findings. Notwithstanding, the current experimental approach convincingly indicates that IH mimicking the episodic hypoxia of sleep apnea induces adipose tissue dysfunction, macrophage infiltration, and phenotypic shift, as well as insulin resistance, all of which are ameliorated by administration of Resv.

Notably, although Resv treatment did not completely restore the overall reduced food intake and weight gain associated with IH, it reversed both systemic and insulin resistance. Thus, the potential use of Resv as a dietary supplement in patients with OSA who also manifest subclinical evidence of insulin resistance may ultimately improve metabolic control and potentially prevent the increased incidence of diabetes in this population (20). Furthermore, the beneficial impact of Resv on the inflam-

matory phenotype of the SVF of 2 VWAT depots would suggest that the increased activation of inflammatory pathways elicited by IH (18, 49) was reversed by administration of Resv. Notably the effects of IH and those of Resv treatment were remarkably similar in both adipose tissue depots. We here not only explored a previously described inflammatory pathway, namely macrophages, but also their polarity shifts. The compelling evidence supporting a major role for adipose tissue macrophage infiltration in the context of obesity and metabolic derangements is mimicked by chronic IH in the absence of an obesogenic diet. We can further infer based on the putative roles of macrophage phenotypes (50) that the magnitude of the primarily M1 macrophage infiltration, along with the reciprocal M2 macrophage reduction, is a major determinant of the degree of insulin resistance induced by long-term IH (51–55). Indeed, concurrent with the increased presence of macrophages in IH-exposed adipose tissues, a phenomenon that may be mediated by transcription factors such as hypoxia-inducible factors or nuclear factor κB (27, 48, 56), there was also a shift in their phenotypes, such that increased populations of M1 macrophages along with reduced M2 macrophage cell counts occurred and were reversed by administration of Resv.

Thus, our current findings conclusively confirm that chronic IH, a frequent occurrence in the context of OSA and other respiratory diseases, is an important contributor to the metabolic dysfunction associated with these disorders, most likely via effects on visceral adipose tissue, even when food intake is reduced. Furthermore, we have shown that concurrent administration of Resv improves the reductions in food intake and weight gain and is particularly effective at reversing the metabolic disturbances induced by IH, most likely by abrogating visceral adipose tissue inflammation. Thus, regular use of dietary supplements, such as Resv, may provide a useful adjunct therapy aimed at reducing the early stages of metabolic dysfunction in OSA.

Acknowledgments

Address all correspondence and requests for reprints to: David Gozal, Department of Pediatrics, Pritzker School of Medicine, The University of Chicago, 5721 South. Maryland Avenue, MC8000, K160, Chicago, IL 60637-1470. E-mail: dgozal@uchicago.edu.

This work was supported by the Herbert T. Abelson Endowed Chair in Pediatrics (D.G.).

Disclosure Summary: The authors have nothing to disclose.

References

1. **Li RC, Row BW, Kheirandish L, et al.** Nitric oxide synthase and intermittent hypoxia-induced spatial learning deficits in the rat. *Neurobiol Dis*. 2004;17(1):44–53.
2. **Veasey SC, Davis CW, Fenik P, et al.** Long-term intermittent hypoxia in mice: protracted hypersomnolence with oxidative injury to sleep-wake brain regions. *Sleep*. 2004;27(2):194–201.
3. **Nair D, Dayyat EA, Zhang SX, Wang Y, Gozal D.** Intermittent hypoxia-induced cognitive deficits are mediated by NADPH oxidase activity in a murine model of sleep apnea. *PLoS One*. 2011;6(5):e19847.
4. **Kheirandish L, Row BW, Li RC, Brittian KR, Gozal D.** Apolipoprotein E-deficient mice exhibit increased vulnerability to intermittent hypoxia-induced spatial learning deficits. *Sleep*. 2005;28(11):1412–1417.
5. **Davis EM, O'Donnell CP.** Rodent models of sleep apnea. *Respir Physiol Neurobiol*. 2013;188(3):355–361.
6. **Chou YT, Zhan G, Zhu Y, et al.** C/EBP homologous binding protein (CHOP) underlies neural injury in sleep apnea model. *Sleep*. 2013;36(4):481–492.
7. **Fang G, Song D, Ye X, Mao SZ, Liu G, Liu SF.** Chronic intermittent hypoxia exposure induces atherosclerosis in ApoE knockout mice: role of NF-κB p50. *Am J Pathol*. 2012;181(5):1530–1539.
8. **Schulz R, Murzabekova G, Egemnazarov B, et al.** Arterial hypertension in a murine model of sleep apnea: role of NADPH oxidase 2. *J Hypertens*. 2014;32(2):300–305.
9. **Chalacheva P, Thum J, Yokoe T, O'Donnell CP, Khoo MC.** Development of autonomic dysfunction with intermittent hypoxia in a lean murine model. *Respir Physiol Neurobiol*. 2013;188(2):143–151.
10. **Gautier-Veyret E, Arnaud C, Bäck M, et al.** Intermittent hypoxia-activated cyclooxygenase pathway: role in atherosclerosis. *Eur Respir J*. 2013;42(2):404–413.
11. **Iiyori N, Alonso LC, Li J, et al.** Intermittent hypoxia causes insulin resistance in lean mice independent of autonomic activity. *Am J Respir Crit Care Med*. 2007;175(8):851–857.
12. **Li J, Savransky V, Nanayakkara A, Smith PL, O'Donnell CP, Polotsky VY.** Hyperlipidemia and lipid peroxidation are dependent on the severity of chronic intermittent hypoxia. *J Appl Physiol (1985)*. 2007;102(2):557–563.
13. **Drager LF, Li J, Reinke C, Bevans-Fonti S, Jun JC, Polotsky VY.** Intermittent hypoxia exacerbates metabolic effects of diet-induced obesity. *Obesity (Silver Spring)*. 2011;19(11):2167–2174.
14. **Gharib SA, Khalyfa A, Abdelkarim A, et al.** Intermittent hypoxia activates temporally coordinated transcriptional programs in visceral adipose tissue. *J Mol Med (Berl)*. 2012;90(4):435–445.
15. **Carreras A, Kayali F, Zhang J, Hirotsu C, Wang Y, Gozal D.** Metabolic effects of intermittent hypoxia in mice: steady versus high-frequency applied hypoxia daily during the rest period. *Am J Physiol Regul Integr Comp Physiol*. 2012;303(7):R700–R709.
16. **Lee EJ, Alonso LC, Stefanovski D, et al.** Time-dependent changes in glucose and insulin regulation during intermittent hypoxia and continuous hypoxia. *Eur J Appl Physiol*. 2013;113(2):467–478.
17. **Jun JC, Shin MK, Yao Q, et al.** Acute hypoxia induces hypertriglyceridemia by decreasing plasma triglyceride clearance in mice. *Am J Physiol Endocrinol Metab*. 2012;303(3):E377–E388.
18. **Poulain L, Thomas A, Rieusset J, et al.** Visceral white fat remodelling contributes to intermittent hypoxia-induced atherogenesis. *Eur Respir J*. 2014;43(2):513–522.
19. **Gozal D, Capdevila OS, Kheirandish-Gozal L.** Metabolic alterations and systemic inflammation in obstructive sleep apnea among nonobese and obese prepubertal children. *Am J Respir Crit Care Med*. 2008;177(10):1142–1149.
20. **Kendzerska T, Gershon AS, Hawker G, Tomlinson G, Leung RS.** Obstructive sleep apnea and incident diabetes. A historical cohort study. *Am J Respir Crit Care Med*. 2014;190(2):218–225.
21. **Guest JF, Panca M, Sladkevicius E, Taheri S, Stradling J.** Clinical outcomes and cost-effectiveness of continuous positive airway pressure to manage obstructive sleep apnea in patients with type 2 diabetes in the U.K. *Diabetes Care*. 2014;37(5):1263–1271.
22. **Zhong W, Tang YG, Zhao X, Go FY, Harper RM, Hui H.** Treating

obstructive sleep apnea with continuous positive airway pressure benefits type 2 diabetes management. *Pancreas*. 2014;43(3):325–330.
23. **Grimaldi D, Beccuti G, Touma C, Van Cauter E, Mokhlesi B.** Association of obstructive sleep apnea in rapid eye movement sleep with reduced glycemic control in type 2 diabetes: therapeutic implications. *Diabetes Care*. 2014;37(2):355–363.
24. **Louis M, Punjabi NM.** Effects of acute intermittent hypoxia on glucose metabolism in awake healthy volunteers. *J Appl Physiol (1985)*. 2009;106(5):1538–1544.
25. **Yokoe T, Alonso LC, Romano LC, et al.** Intermittent hypoxia reverses the diurnal glucose rhythm and causes pancreatic β-cell replication in mice. *J Physiol*. 2008;586(3):899–911.
26. **Xu J, Long YS, Gozal D, Epstein PN.** β-Cell death and proliferation after intermittent hypoxia: role of oxidative stress. *Free Radic Biol Med*. 2009;46(6):783–790.
27. **Fang Y, Zhang Q, Tan J, Li L, An X, Lei P.** Intermittent hypoxia-induced rat pancreatic β-cell apoptosis and protective effects of antioxidant intervention. *Nutr Diabetes*. 2014;4:e131.
28. **Zhang SX, Qiao Z, Gozal D, Wang Y.** Intermittent hypoxia-induced metabolic dysfunction in visceral fat is associated with immune deregulation and inflammation. *Am J Respir Crit Care Med* 2013; 187:2013:A2383.
29. **Eguchi J, Kong X, Tenta M, Wang X, Kang S, Rosen ED.** Interferon regulatory factor 4 regulates obesity-induced inflammation through regulation of adipose tissue macrophage polarization. *Diabetes*. 2013;62(10):3394–403.
30. **Polak J, Shimoda LA, Drager LF, et al.** Intermittent hypoxia impairs glucose homeostasis in C57BL6/J mice: partial improvement with cessation of the exposure. *Sleep*. 2013;36(10):1483–1490; 1490A–1490B.
31. **He Q, Yang QC, Zhou Q, et al.** Effects of varying degrees of intermittent hypoxia on proinflammatory cytokines and adipokines in rats and 3T3-L1 adipocytes. *PLoS One*. 2014;9(1):e86326.
32. **Olea E, Agapito MT, Gallego-Martin T, et al.** Intermittent hypoxia and diet-induced obesity: effects on oxidative status, sympathetic tone, plasma glucose and insulin levels and arterial pressure. *J Appl Physiol (1985)*. 2014;117(7):706–719.
33. **Pearson KJ, Baur JA, Lewis KN, et al.** Resveratrol delays age-related deterioration and mimics transcriptional aspects of dietary restriction without extending life span. *Cell Metab*. 2008;8:157–168.
34. **Baur JA, Pearson KJ, Price NL, et al.** Resveratrol improves health and survival of mice on a high-calorie diet. *Nature*. 2006;444:337–342.
35. **Lagouge M, Argmann C, Gerhart-Hines Z, et al.** Resveratrol improves mitochondrial function and protects against metabolic disease by activating SIRT1 and PGC-1α. *Cell*. 2006;127:1109–1122.
36. **Baur JA, Sinclair DA.** Therapeutic potential of resveratrol: the in vivo evidence. *Nat Rev Drug Discov*. 2006;5:493–506.
37. **Um JH, Park SJ, Kang H, et al.** AMP-activated protein kinase-deficient mice are resistant to the metabolic effects of resveratrol. *Diabetes*. 2010;59(3):554–563.
38. **Price NL, Gomes AP, Ling AJ, et al.** SIRT1 is required for AMPK activation and the beneficial effects of resveratrol on mitochondrial function. *Cell Metab*. 2012;15(5):675–690.
39. **Nwachukwu JC, Srinivasan S, Bruno NE, et al.** Resveratrol modulates the inflammatory response via an estrogen receptor-signal integration network. *Elife*. 2014;3:e02057.
40. **Gozal D, Daniel JM, Dohanich GP.** Behavioral and anatomical correlates of chronic episodic hypoxia during sleep in the rat. *J Neurosci*. 2001;21:2442–2450.
41. **Sargis RM, Neel BA, Brock CO, et al.** The novel endocrine disruptor tolylfluanid impairs insulin signaling in primary rodent and human adipocytes through a reduction in insulin receptor substrate-1 levels. *Biochim Biophys Acta*. 2012;1822:952–960.
42. **van den Borst B, Schols AM, de Theije C, et al.** Characterization of the inflammatory and metabolic profile of adipose tissue in a mouse model of chronic hypoxia. *J Appl Physiol (1985)*. 2013;114(11): 1619–1628.
43. **Zhang H, Zhang G, Gonzalez FJ, Park SM, Cai D.** Hypoxia-inducible factor directs POMC gene to mediate hypothalamic glucose sensing and energy balance regulation. *PLoS Biol*. 2011;9(7): e1001112.
44. **Schneider Y, Duranton B, Gossé F, Schleiffer R, Seiler N, Raul F.** Resveratrol inhibits intestinal tumorigenesis and modulates host-defense-related gene expression in an animal model of human familial adenomatous polyposis. *Nutr Cancer*. 2001;39:102–107.
45. **Norata GD, Marchesi P, Passamonti S, Pirillo A, Violi F, Catapano AL.** Anti-inflammatory and anti-atherogenic effects of cathechin, caffeic acid and trans-resveratrol in apolipoprotein E deficient mice. *Atherosclerosis*. 2007;191:265–271.
46. **Qureshi AA, Guan XQ, Reis JC, et al.** Inhibition of nitric oxide and inflammatory cytokines in LPS-stimulated murine macrophages by resveratrol, a potent proteasome inhibitor. *Lipids Health Dis*. 2012; 11:76.
47. **Cho SJ, Jung UJ, Choi MS.** Differential effects of low-dose resveratrol on adiposity and hepatic steatosis in diet-induced obese mice. *Br J Nutr*. 2012;108:2166–2175.
48. **Taylor CT, Kent BD, Crinion SJ, McNicholas WT, Ryan S.** Human adipocytes are highly sensitive to intermittent hypoxia induced NF-κB activity and subsequent inflammatory gene expression. *Biochem Biophys Res Commun*. 2014;447(4):660–665.
49. **Reinke C, Bevans-Fonti S, Drager LF, Shin MK, Polotsky VY.** Effects of different acute hypoxic regimens on tissue oxygen profiles and metabolic outcomes. *J Appl Physiol (1985)*. 2011;111(3):881–890.
50. **Vieira-Potter VJ.** Inflammation and macrophage modulation in adipose tissues. *Cell Microbiol*. 2014;16(10):1484–1492.
51. **Charo IF.** Macrophage polarization and insulin resistance: PPARγ in control. *Cell Metab*. 2007;6(2):96–98.
52. **Weisberg SP, McCann D, Desai M, Rosenbaum M, Leibel RL, Ferrante AW Jr.** Obesity is associated with macrophage accumulation in adipose tissue. *J Clin Invest*. 2003;112:1796–1808.
53. **Di Gregorio GB, Yao-Borengasser A, Rasouli N, et al.** Expression of CD68 and macrophage chemoattractant protein-1 genes in human adipose and muscle tissues: association with cytokine expression, insulin resistance, and reduction by pioglitazone. *Diabetes*. 2005; 54:2305–2313.
54. **Oh DY, Morinaga H, Talukdar S, Bae EJ, Olefsky JM.** Increased macrophage migration into adipose tissue in obese mice. *Diabetes*. 2012;61(2):346–354.
55. **Hernandez ED, Lee SJ, Kim JY, et al** Macrophage NBR1-MEKK3 complex triggers JNK-mediated adipose tissue inflammation in obesity. *Cell Metab*. 2014;20(3):499–511.
56. **Fujisaka S, Usui I, Ikutani M, et al.** Adipose tissue hypoxia induces inflammatory M1 polarity of macrophages in an HIF-1α-dependent and HIF-1α-independent manner in obese mice. *Diabetologia*. 2013;56(6):1403–1412.